On Point-wise Models for MIMO Wireless Systems

Leif W. Hanlen
National ICT Australia†
Canberra, Australia

Minyue Fu
School of Electrical Engineering & Computer Science
The University of Newcastle, Australia

***Abstract*— We consider the standard (point-wise) linear channel model for MIMO wireless systems in terms of a continuous operator channel. We show analytically that the point-wise representation over-estimates the (true) modal connection strengths and produces artificially distorted channel singular values. Analytic results are compared with simulations for simple channel models and the convergence of the point-wise model toward the continuous model is shown.**

I. Introduction

The advent of multiple-input multiple-output (MIMO) wireless communications has promoted the concept of high bandwidth wireless systems employing large numbers of antenna elements at the transmit and receive ends of the wireless link. To accommodate user mobility, a great deal of interest has been devoted to closely spaced array elements and the effects of correlation for small wireless devices. Much of the wireless communication literature uses a linear, spatial model which is based upon an abstraction of antenna elements to points in space. We refer to such models as *point-wise models.*

The discrete-point abstraction of antenna elements is valid for well separated elements and is supported by a large amount of measurement data [1]. Unfortunately, as the antenna elements become closely spaced, the point-wise modelling techniques become hidden under the application of correction factors – such as correlation matrices or norm adjustments [2] – which attempt to account for close proximity of elements and effects such as mutual coupling.

Recent work [2–5] has shown that spatially diverse wireless systems may be modelled using *continuous spatial* techniques, which focus on the continuous nature of space, rather than the individual antenna elements. In particular, it has been shown that a single user wireless channel is limited by the *region enclosing the antenna arrays, not the number of elements in the array [4, 5].* Although orthonormal expansions [3] may be used to model *arbitrary* antenna arrays and elements they lack the simplicity of the point-wise matrix model. In [6] it was shown that antenna elements may be seen as "samples" of the continuous channel. It is natural to ask how well we may estimate the continuous channel given only the point-wise matrix entries and rudimentary details of the regions enclosing the antenna arrays. *Can we reconcile the simplicity of point-wise MIMO vector models* e.g., *[7], with the fundamental benefits of continuous spatial techniques?*

[0]† National ICT Australia is funded through the Australian Government's *Backing Australia's Ability* initiative, in part through the Australian Research Council

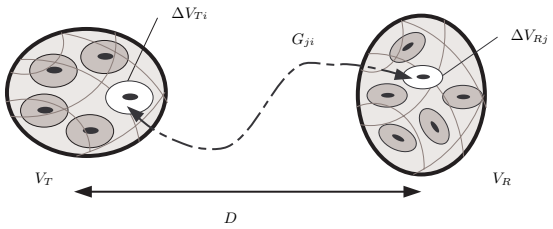

Fig. 1: Continuous solid regions V_T (transmit) and V_R (receive) containing N_t and N_r discrete antenna elements respectively. Two particular elements are highlighted, with the corresponding channel matrix entry G_{ji} shown. figure

In this paper we show that the point-wise approximation of the continuous channel may be interpreted as a particular choice of orthonormal expansion. However, this "discrete" sequence is a poor choice for basis expansion as it;

1) over-estimates the continuous mode strengths and
2) has no equivalent "sum-rule" (c.f. [8]) accuracy measure.

The estimation error described in point 1 may be reduced, at the expense of using a large number of sampling points[1]. The main result of this paper is that we may adopt the simpler point-wise approach for MIMO, if we are willing to accept *an artificially correlated estimate of the channel.*

This paper is arranged as follows: in section II we describe the continuous space channel model and compare with the point-wise model of the open literature. In section III we show analytically that the point-wise model *over-estimates* the connection strengths of the continuous case and has no measure of representational accuracy. Section IV presents numerical comparisons of the two modelling techniques and shows that the point-wise approach is inaccurate in determining channel eigenvalues. We draw conclusions in section V.

II. Channel Model

Consider the physical arrangement shown in Fig 1. We have shown two regions V_T and V_R in space which communicate with each other over a given channel – which may or may not contain scatterers. The region V_T contains N_t sources (transmit elements) which produce a signal within V_R, and V_R contains N_r receive elements. We have superimposed "discrete" antenna elements contained within each region, shown as black spots in Fig 1. Each (transmit/receive) element

[1]Although estimating continuous functions via discrete points is inefficient [9, 10], our main argument is that the point-wise model will produce artificial estimates of channel correlation.

may be considered as the centroid of a given sub-region. The i^{th} transmit element is located at a point $\rho_{Ti} \in V_T$ and may be considered as being contained by the small sub-region ΔV_{Ti} as shown. Each sub-region ΔV_{Ti} is assumed to be disjoint and the collection of sub-regions occupies the whole of V_T, *i.e.,* $V_T = \sum_i \Delta V_{Ti}$. Similarly, the receive elements are contained within small disjoint sub-regions ΔV_{Rj} whose collective occupies all of V_R.

The enclosing regions V_T and V_R are separated by a distance D (between their centers) which is assumed to be large compared to their volumes. This corresponds to the typical case for indoor and outdoor wireless transmission, where a base-station communicates with a mobile receiver over (at least) a small number of meters. We shall assume that the channel is single-frequency, has no inter-symbol interference and is time-invariant. We shall not be interested in electro-magnetic field modelling, rather we consider the MIMO channel estimate: We assume that each transmit and receive element does not interact with the (scalar) electrical field *as is assumed in the MIMO literature we are contrasting with.* Removing this assumption will make the point-wise model more accurate, at the expense of EM-modelling.

We shall consider functions $\psi(\mathbf{r}_T)$ for points $\mathbf{r}_T \in V_T$ where $\mathbf{r}_T = \{x, y, z\}$ is a vector in 3-space. The inner product of two such functions $\psi(\mathbf{r}_T)$ and $f(\mathbf{r}_T)$, is defined:

$$\langle \psi | f \rangle_{V_T} \triangleq \int_{V_T} \psi(\mathbf{r}) \overline{f(\mathbf{r})}\, d\mathbf{r} \tag{1}$$

where $\overline{x}$ denotes complex conjugate and the integral of (1) is a volume integral. We shall assume that the functions $\psi(\mathbf{r}_T)$ are sufficiently well behaved to ensure a valid inner product. The functions $\psi(\mathbf{r}_T)$ may be considered as transmit signals, which induce receive signals $\phi(\mathbf{r}_R)$ in V_R. We wish to examine the channel connecting transmit and receive signals. If we take any complete, orthonormal sequence of functions $\{\varphi_{Ti}(\mathbf{r}_T)\}_{i=1}^{\infty}$, we may expand signals $\psi(\mathbf{r}_T)$, as coefficients

$$\psi(\mathbf{r}_T) = \sum_i^{\infty} a_i \varphi_{Ti}(\mathbf{r}_T) \qquad a_i \triangleq \langle \psi | \varphi_{Ti} \rangle_{V_T} \tag{2}$$

within the transmit volume V_T, where $\langle \cdot | \cdot \rangle$ denotes inner product. We may apply a similar result for functions $\phi(\mathbf{r}_R)$ in the receive volume V_R, using a complete orthonormal sequence $\{\varphi_{Rj}(\mathbf{r}_R)\}_{j=1}^{\infty}$ and inner product defined over $\mathbf{r}_R \in V_R$. If we write a transmit signal as a vector of Fourier coefficients, $\mathbf{a} = \{a_1, \ldots, a_k, \ldots\}$ and the received signal as a similar vector $\mathbf{b} = \{b_1, \ldots, b_k, \ldots\}$ we may write a linear vector channel of the form:

$$\mathbf{b} = \Gamma \mathbf{a} + \omega \tag{3}$$

where $\mathbf{a}$ is an (infinitely long) input vector, $\mathbf{b}$ is an (infinitely long) output vector, ω is a vector of noise samples and Γ is a communication operator:

$$\phi(\mathbf{r}_R) = (\Gamma\psi)(\mathbf{r}_T) = \int_{V_T} G(\mathbf{r}_R, \mathbf{r}_T) \psi(\mathbf{r}_T)\, d\mathbf{r}_T \tag{4}$$

$$\Gamma_{ji} \triangleq \left\langle \langle G(\mathbf{r}_R, \mathbf{r}_T) | \varphi_{Ti} \rangle_{V_T} | \varphi_{Rj} \right\rangle_{V_R} \tag{5}$$

for a given "connecting" function $G(\mathbf{r}_R, \mathbf{r}_T)$ defined over points in each region. The operator Γ, takes functions from V_T, and produces functions in V_R, according to the properties of the channel. The entries Γ_{ji} may be considered as the *connection strength* between transmit basis function $\varphi_{Ti}(\mathbf{r}_T)$ and receive basis function $\varphi_{Rj}(\mathbf{r}_R)$ for arbitrary choice of functions. The entries Γ_{ji} are determined by the choice of orthonormal sequences while the eigenvalues of Γ are independent of the sequences and represent fundamental properties of the channel.

The operator Γ, is a particular example of a Hilbert-Schmidt operator. Such operators are known to be compact and have finite Frobenius norm cf. [11]:

$$\mathrm{tr}\left(\Gamma\Gamma^*\right) = \|\Gamma\|_F \leq \int_{V_R}\int_{V_T} |G(\mathbf{r}_R, \mathbf{r}_T)|^2\, d\mathbf{r}_R\, d\mathbf{r}_T = \gamma \tag{6}$$

where $\mathrm{tr}\,(\cdot)$ denotes trace and the right-hand side of (6) is dependent on the size of the volumes and the intervening channel. The result of (6) is called a "sum-rule" in [8]. Further, (6) holds with equality (by Parseval's theorem) if and only if the orthonormal sequences of (5) are complete.

The matrix form of Γ will be infinite dimensional, Γ is $n \times n$ with $n \to \infty$, although only a finite number of eigenvalues will have non-negligible magnitude, *i.e.,* although Γ is infinite dimensional, it is effectively finite rank. We denote the number of non-negligible eigenvalues as N_c, which represents the number of communication modes of the particular channel.

We shall compare the well-known point-wise channel model with this operator viewpoint. Recall the point-wise linear channel as defined according to points within the transmit and receive regions. Each element in V_T transmits a signal *independently* of the other elements and the superimposed ensemble is received by elements in V_R. The linear channel may be described in the familiar matrix form:

$$y = Gx + w \tag{7}$$

where x is a vector $x \in \mathbb{C}^{1\times N_t}$, of input signals, defined at points $\rho_{Ti} \in V_T$, G is the $N_t \times N_r$ matrix $G \in \mathbb{C}^{N_t \times N_r}$, of channel coefficients between each transmit-receive pair, y is a vector $y \in \mathbb{C}^{1\times N_r}$ of received signals defined at points $\rho_{Rj} \in V_R$, and w is a vector $y \in \mathbb{C}^{1\times N_r}$, of noise. In direct transmission (no scattering) the entries of G are given by the distance between points $D^0_{ji} = |\rho_{Rj} - \rho_{Ti}|$:

$$G^0_{ji} \triangleq \frac{\exp\left\{-\imath \frac{2\pi}{\lambda} D^0_{ji}\right\}}{4\pi D^0_{ji}} \tag{8}$$

where $\imath = \sqrt{-1}$. Any coupling between transmit elements is given by the matrix G. Scattering may be easily accommodated by noting that each scattering object introduces an additional transmission path – which may be considered separately to all others – with corresponding alteration in the path length: D^k_{ji} is the distance from ρ_{Ti} to ρ_{Rj} along the scattering path. In this way, G may be written as a summation of several paths: $G = \sum_k \alpha_k G^k$ where α_k denotes the path gain for a particular scatter path. Several methods exist for generating such channel matrices in the open literature.

III. Estimation of Γ from G

It is clear that $G(\mathbf{r}_R, \mathbf{r}_T) = G(\rho_{Rj}, \rho_{Ti}) = G_{ji}$ when the points ρ_{Ti} and ρ_{Rj}, coincide with the vectors $\mathbf{r}_T$ and $\mathbf{r}_R$ respectively. We may consider the continuous function $G(\mathbf{r}_R, \mathbf{r}_T)$ a limiting case as the number of transmit and receive points in each region approaches infinity, *i.e.,* $G \equiv G(\mathbf{r}_R, \mathbf{r}_T)$ for $N_t, N_r \to \infty$. It is not sufficient to have G_{ji} approximate the connecting function $G(\mathbf{r}_R, \mathbf{r}_T)$, rather we require the singular values of G and Γ to converge. We shall shortly show that the convergence is not monotonic.

Problem 1 (Estimating Γ given G). *What $N_t \times N_r$ matrix $\widehat{G} = \alpha G$ for some scalar α, approximates Γ? How well do the singular values of $\sigma^{\widehat{G}}$, of $\widehat{G}$, estimate the singular values σ^{Γ}, of the continuous transfer matrix Γ?*

We shall begin by defining sets of functions $\vartheta_{Ti}(\mathbf{r}_T)$ and $\vartheta_{Rj}(\mathbf{r}_R)$ in V_T and V_R respectively, which are constant within the sub-region surrounding antenna element i (resp. j). The functions provide a mapping from the point-wise entries of G to the connection strength entries of Γ. We note that they are not sampling functions: any coupling, polarity effects, etc may be modelled through the use of additional "spatial sampling signatures." The sequences $\{\vartheta_{Ti}(\mathbf{r}_T)\}_{i=1}^{N_t}$ and $\{\vartheta_{Rj}(\mathbf{r}_R)\}_{j=1}^{N_r}$ are not complete for finite N_t and N_r. Define

$$\vartheta_{Ti}(\mathbf{r}_T) = \begin{cases} \frac{1}{\sqrt{\Delta V_{Ti}}} & \mathbf{r}_T \in \Delta V_{Ti} \subseteq V_T \\ 0 & \text{otherwise} \end{cases} \tag{9}$$

where the constant $1/\sqrt{\Delta V_{Ti}}$ is chosen to ensure $\|\vartheta_{Ti}\| = 1$. The ϑ_{Ti} are scaled block functions – constant within ΔV_{Ti} and zero everywhere else. Similarly, we define

$$\vartheta_{Rj}(\mathbf{r}_R) = \begin{cases} \frac{1}{\sqrt{\Delta V_{Rj}}} & \mathbf{r}_R \in \Delta V_{Rj} \subseteq V_R \\ 0 & \text{otherwise} \end{cases} \tag{10}$$

Under the condition that the sub-regions are disjoint, then orthogonality of the sequences $\{\vartheta_{Ti}\}_{i=1}^{N_t}$ and $\{\vartheta_{Rj}\}_{j=1}^{N_r}$ is guaranteed. Using the orthonormal functions from (9) and (10) with the inner product (5) we may generate a particular $N_t \times N_r$ instantiation of Γ by:

$$\Gamma_{ji} \triangleq \frac{1}{\sqrt{\Delta V_{Rj}\Delta V_{Ti}}} \int_{\Delta V_{Rj}} \int_{\Delta V_{Ti}} G(\mathbf{r}_R, \mathbf{r}_T)\, d\mathbf{r}_R\, d\mathbf{r}_T \tag{11}$$

If the sub-regions ΔV_{Ti} and ΔV_{Rj}, are sufficiently small, then the integrand of (11) may be approximated as a constant throughout both sub-regions. In this case the integrand is independent of the variables of integration and the connectivity strength between $\vartheta_{Ti}(\mathbf{r}_T)$ and $\vartheta_{Rj}(\mathbf{r}_R)$ is given by a complex scalar.

$$\Gamma_{ji} \approx \widehat{G}_{ji} = G(\rho_{Rj}, \rho_{Ti}) \cdot \sqrt{\Delta V_{Rj}\Delta V_{Ti}} \tag{12}$$

$$= G_{ji} \cdot \sqrt{\Delta V_{Rj}\Delta V_{Ti}} \tag{13}$$

where the approximation of (12) is accurate if the sub-regions are *sufficiently* small. From (13), the point-wise transfer matrix G will have a scaling offset of the true connection strength estimates. If we assume that all the sub-regions are equal in size, then $\Delta V_{Ti} = V_T/N_t$ and $\Delta V_{Rj} = V_R/N_r$, where we have denotated the volume of the solid regions as V_T and V_R respectively. We may re-write (13)

$$\widehat{G} = G\sqrt{\frac{V_T V_R}{N_t N_r}} = \alpha G \tag{14}$$

The result of (14) recalls the scaling factor[2] applied in [7] and the "Frobenius norm" scaling applied in [12]. Note that we have not used physical constraints to justify this scaling, it is a result of using orthonormal functions. However, the entries of $\widehat{G}$ *over-estimate* the entries of Γ. This error diminishes to zero as the sampling points become sufficiently dense.

Lemma 1. *The entries of the $N_t \times N_r$ (point-wise) estimation matrix $\widehat{G}$ have a larger magnitude than the equivalent entries of the $N_t \times N_r$ continuous channel matrix Γ for finite N_t and N_r.*

Proof. Consider $|\Gamma_{ji}|$ from (11) and the corresponding entry $|\widehat{G}_{ji}|$.

$$|\Gamma_{ji}| \leq \frac{\int_{\Delta V_{Rj}} \int_{\Delta V_{Ti}} |G(\mathbf{r}_R, \mathbf{r}_T)|\, d\mathbf{r}_R\, d\mathbf{r}_T}{\sqrt{\Delta V_{Rj}\Delta V_{Ti}}} \leq |\widehat{G}_{ji}|$$

which results from the triangle inequality [11]. □

If we view the estimate (13) as a trapezoidal approximation of the integral (11), then the error is of order $\mathcal{O}\left\{\max\left(\Delta V_{Ti} + \Delta V_{Rj}\right)^2 \cdot G'(\mathbf{r}_R, \mathbf{r}_T)\right\}$ where $G'(\mathbf{r}_R, \mathbf{r}_T)$ is the derivative of $G(\mathbf{r}_R, \mathbf{r}_T)$ evaluated at an unknown point [10, pp.133] which implies the estimation error diminishes as the sub-volumes become small although the exact error is unknown. For any finite N_t, N_r the orthonormal sequences $\{\vartheta_{Ti}\}_{i=1}^{N_t}$ and $\{\vartheta_{Rj}\}_{j=1}^{N_r}$ are not complete and (6) will remain an inequality. As such

$$\|\Gamma\|_F = \mathrm{tr}\left(\Gamma\Gamma^*\right) \leq \gamma \tag{15}$$

we may also see that

$$\mathrm{tr}\left(\widehat{G}\widehat{G}^*\right) = \sum_{i}^{N_t}\sum_{j}^{N_r} |G_{ji}|^2 \Delta V_{Ti}\Delta V_{Rj} \approx \gamma \tag{16}$$

for any value of N_t, N_r. This is due to the inaccuracy of approximating an integral with a scaled sample. However, (16) shows **there is no equivalent sum-rule for the point-wise estimation case.** As such, we cannot tell (from the entries of $\widehat{G}$ alone) whether the representation of $\widehat{G}$ is a sufficiently accurate estimate of Γ.

Lemma 1 implies that the point-wise matrix model for MIMO channels is a biased estimator for the continuous channel eigenvalues. We may approximate the bias as follows. If each entry of $\widehat{G}$ is offset by a similar error, which holds if the sub-regions are small and equal size, then we may write $\widehat{G}$ as:

$$\widehat{G} \approx \Gamma + \epsilon\mathbf{1} \cdot \sqrt{\gamma - \mathrm{tr}\left(\Gamma\Gamma^*\right)} \tag{17}$$

[2] In [7] the elements were assumed to be dense at the receiver only, so that only a factor of $\sqrt{V_R/N_r}$ was applied, with $V_R = 1$.

where $\mathbf{1}$ is a rank one matrix and ϵ is an arbitrary constant.

The form of (17) implies that **the conditioning of $\widehat{G}$ will be artificially worse than Γ due to the over-estimation error.** The low-order singular values of $\widehat{G}$ will be larger than their counterparts in Γ: $|\sigma_1^{\widehat{G}}| \geq |\sigma_1^{\Gamma}|$, and the high-order singular values of $\widehat{G}$ will be correspondingly smaller than those of Γ: $|\sigma_n^{\widehat{G}}| \leq |\sigma_n^{\Gamma}|$. This means a point-wise MIMO channel will appear *artificially correlated* compared with its continuous counterpart, implying that signal designs based on the point-wise technique will have lower capacity than those using knowledge of the continuous channel.

IV. Numerical Results

We shall present simple channels which emphasize the convergence of the point-wise modelling approach, the results are equally valid for more complex channels. We have considered two transmission scenarios: 1) direct (no multipath) between large volumes, 2) between thin plates in non-line of sight multi-path.

For the direct transmission case we chose V_T and V_R to be identical cubes of side length 20λ and a transmission frequency of $3GHz$, giving $\lambda = 0.1m$. The cubes were separated (center-to-center) by $D = 100\lambda$ along the z-axis and had their edges aligned along the x, y, z axes. We used equal numbers of sub-regions along each dimension. For 3-space this means that $N_t = N_r = {N_{\text{sam}}}^3$ where N_{sam} is the number of samples along a single dimension. The number of well connected modes [8] is

$$N_c = \frac{A_T A_R}{D^2\lambda^2} = \frac{(20\lambda)^2(20\lambda)^2}{D^2\lambda^2} = 16 \qquad (18)$$

A_T is the surface area of the parallel face at V_T and similarly for A_R. The magnitude of the singular values is bounded by:

$$\left|\sigma^{\Gamma}\right|^2 \leq \frac{V_T V_R}{(4\pi D)^2}\frac{1}{N_c} = 2.533 \times 10^{-4} = |\mu|^2 \qquad (19)$$

Fig 2 shows the modes estimated from the point-wise model. For Fig 2(a) one sub-region *i.e.,* $N_t = N_r = 1$ has been used to estimate Γ. It can be seen that the magnitude of the estimated singular value is sixteen times larger than the bound of (19), *i.e.,* $|||\sigma_1^{\widehat{G}}|^2 \approx 16|\mu|^2$. As the number of sub-regions increases, the estimate of the singular value magnitudes improves toward the continuous values, shown in Fig 2(c). In Fig 2(b) we have used $N_t = N_r = 22^3$ samples and the difference between the point-wise estimate and continuous calculation is negligible.

For random scattering two equal sized thin plates were used, $V_T = V_T = 5\lambda \times 5\lambda \times 0.1\lambda$ separated by 20λ along the z-axis. The plates had their edges aligned along the x, y, z axes with faces. Scattering bodies were placed at random, locally to V_T and V_R. Each scattering path consisted of two scattering bodies: from V_T to a local scattering body near V_T, to a local scattering body near V_R and then to V_R. Each scattering body was assumed purely reflective and given a random normal direction as described in [5].

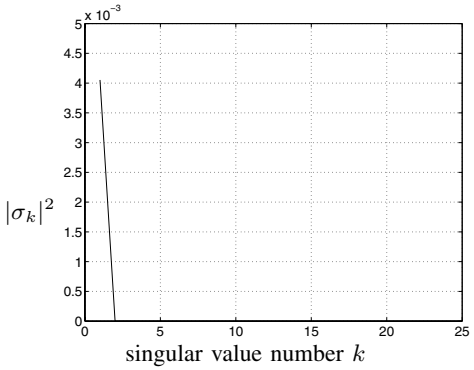

(a) Discrete model, $N_t = N_r = 1$. Note scale.

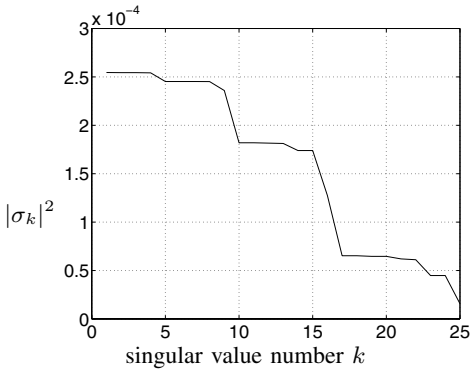

(b) $N_t = N_r = 22^3 = 10648$

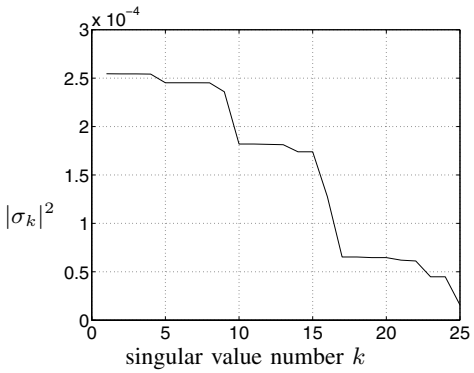

(c) Continuous comparison

Fig. 2: Comparison for point-wise and continuous models for direct transmission between $20\lambda \times 20\lambda \times 20\lambda$ cubes, separated by $D = 100\lambda$, $\lambda = 0.1m$. Number of well-connected modes $N_c = 16$, and eigenvalues bounded by $\left|\sigma^{\Gamma}\right|^2 \leq |\mu|^2$.
figure

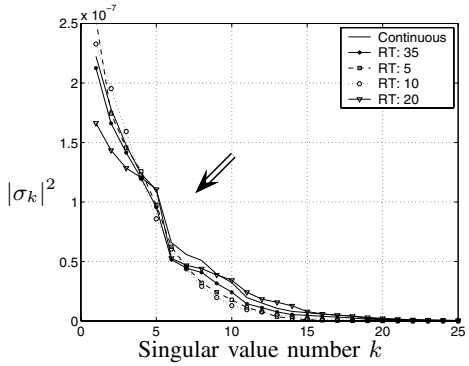

(a) Discrete model convergence, highlighted region (arrow) shows region of magnification in Fig 3(b).

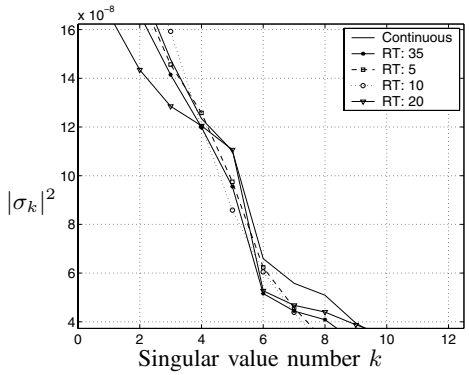

(b) Discrete model convergence with increased scale, examining highlighted region. Corresponding region in Fig 3(a) shown by arrow.

Fig. 3: Singular values for increasing number of sub-regions for point-wise approach.
figure

Figure 3 compares the results for continuous and point-wise models using Monte Carlo simulations. For each iteration a new set of local scatterers was generated and the channel matrices calculated. The process was repeated for 5, 10, 20 and 35 samples per dimension for the point-wise case. The mean singular values magnitudes (squared) for both Γ and $\widehat{G}$ are plotted. The first 25 values are shown in Fig 3(a) and expanded in Fig 3(b). It can be seen that the estimates from point-wise modelling converge to the continuous singular values as the number of sub-regions increases. Even for large numbers of sub-regions, $N_t = N_r = 35^2 = 1225$ the low-order singular values are over-estimated.

A. Computational complexity

The number of samples required to generate reasonable estimates of the continuous channel from the point-wise matrix is very large. It can be seen from Fig 2(b) that $N_t = N_r = {N_{\text{sam}}}^3 = 10648$ samples were required to reasonably approximate Γ. The channel matrix $\widehat{G}$ was then 10648×10648 with only 16 significant singular values. For an $n \times n$ matrix, the singular value decomposition (SVD) algorithm takes $\mathcal{O}(n^3/2)$ operations [9]. This shows that the point-wise model is an inefficient method of representing the continuous channel.

V. Conclusion

As the number of antenna elements within a fixed region of space becomes large, point-wise models converge toward the continuous case after the application of a scale factor. We have shown how this scale factor may be found without need for "power-scaling" arguments. We have shown that the estimates of the continuous connection strengths given by the point-wise channel matrix $\widehat{G}$ are over-estimates of the true channel modes which results in artificially distorted channel matrix singular values, with low-order modes over-estimated and high-order modes under-estimated. This implies that the MIMO point-wise model is a biased estimator of the continuous eigenvalues.

For low estimate errors, the channel matrix $\widehat{G}$ must have large dimension for non-trivial arrangements. Thus direct application of the SVD algorithm to G (or $\widehat{G}$) requires substantial computation and results in only a small number of significant singular values. Numerical techniques which incorporate greater knowledge of the continuous wave functions are likely to show improved computational complexity, and will not require such large numbers of samples to produce reasonable results.

References

[1] K. Yu and B. Ottersten, "Models for MIMO propagation channels: A review," *Wireless Communications and Mobile Computing*, vol. 2, pp. 653–666, Nov. 2002.

[2] J. W. Wallace and M. A. Jensen, "Intrinsic capacity of the MIMO wireless channel," in *IEEE Veh. Technol. Conf. (VTC 2002-Fall)*, Vancouver, Canada, 2002, pp. 701–705.

[3] R. A. Kennedy and T. D. Abhayapala, "Spatial concentration of wavefields: Towards spatial information content in arbitrary multipath scattering," in *4th Aust. Commun. Theory Workshop, AusCTW*, Melbourne, Australia, Feb. 4–5 2003, pp. 38–45.

[4] T. S. Pollock, "On limits of multi-antenna wireless communications in spatially selective channels," Ph.D. dissertation, The Australian National University, July 2003.

[5] L. W. Hanlen, "Channel modelling and capacity analysis for multi-input, multi-output, wireless communication systems," Ph.D. dissertation, The University of Newcastle, June 2003.

[6] M. Fu and L. W. Hanlen, "Capacity of MIMO channels: A volumetric approach," in *Proc. IEEE Intl. Conf. Commun., ICC*, Anchorage, Alaska, May 11–15 2003, pp. 2673–2677.

[7] N. Chiurtu, B. Rimoldi, and E. Telatar, "Dense multiple antenna systems," in *IEEE Inform. Theory Workshop*, Cairns, Australia, Sept. 2–7 2001, pp. 108–109.

[8] D. A. Miller, "Communicating with waves between volumes: evaluating orthogonal spatial channels and limits on coupling strengths," *Applied Optics*, vol. 39, no. 11, pp. 1681–1699, Apr. 2000.

[9] J. Buchanan and P. Turner, *Numerical Methods and Analysis*, ser. International Series in Pure and Applied Mathematics. Singapore: McGraw-Hill, 1992.

[10] W. H. Press, S. A. Teukolsky, W. T. Vetterling, and B. P. Flannery, *Numerical Recipes in C*. Cambridge University Press, 1994.

[11] E. Kreysig, *Introductory functional analysis with applications*. New York, USA: John Wiley & Sons, 1978.

[12] T. Svantesson and J. W. Wallace, "On signal strength and multipath richness in multi-input multi-output systems," in *Proc. IEEE Intl. Conf. Commun., ICC*, Anchorage, Alaska, May 11–15 2003, pp. 2683–2687.